Electronic Supplementary Material (ESI) for Soft Matter.
This journal is © The Royal Society of Chemistry 2018

Electronic Supplementary Information (ESI) on

The influence of plasma treatment on the elasticity of the in-situ oxidized gradient layer in PDMS: Towards crack-free wrinkling

Bernhard Alexander Glatz,[1,2] and Andreas Fery[1,3]*

[1] Institute of Physical Chemistry and Polymer Physics, Leibniz Institute of Polymer Research Dresden e. V., Hohe Str. 6, 01069 Dresden, Germany

[2] University of Bayreuth Graduate School, University of Bayreuth, Universitätsstr. 30, 95477 Bayreuth,

[3] Chair for Physical Chemistry of Polymeric Materials, Technical University Dresden, Mommsenstr. 4, 01062 Dresden, Germany

Corresponding author: e-Mail: fery@ipfdd.de; Phone: +49 351 4658 225; Fax: +49 351 4658 281

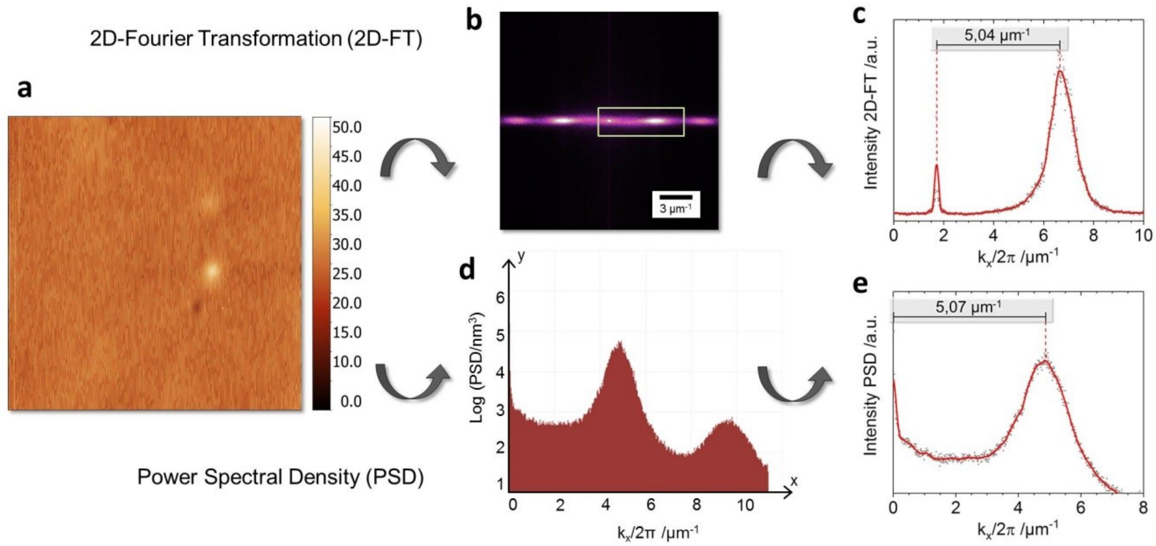

Figure S1: Evaluation process for topographical AFM images (**a**) via 2D-FT and PSD, exemplarily shown for one of the three samples used in the power screening at 4 W (5 % Plasma Cleaner power). For 2D-FT the AFM image is first transformed over a 2-Dimensional Fast Fourier Transformation (2D-FFT) to a FT-spectrum (**b**). In here, the area marked with the white box (including the FT-origin peak and the 1st order peak) is extracted as a profile. The data is fitted in Origin Pro with an FFT-filter (**c**) and the peak positions are subtracted from each other, resulting in the wavenumber k of the according corrugation length observed within the topographical AFM image. For PSD, the horizontal axis of the AFM image gets transformed in NanoScope Analysis software (**d**) and eventually the extracted profile is analyzed similar to 2D-FT (**e**), with the addition that the origin peak is automatically set to x = 0.

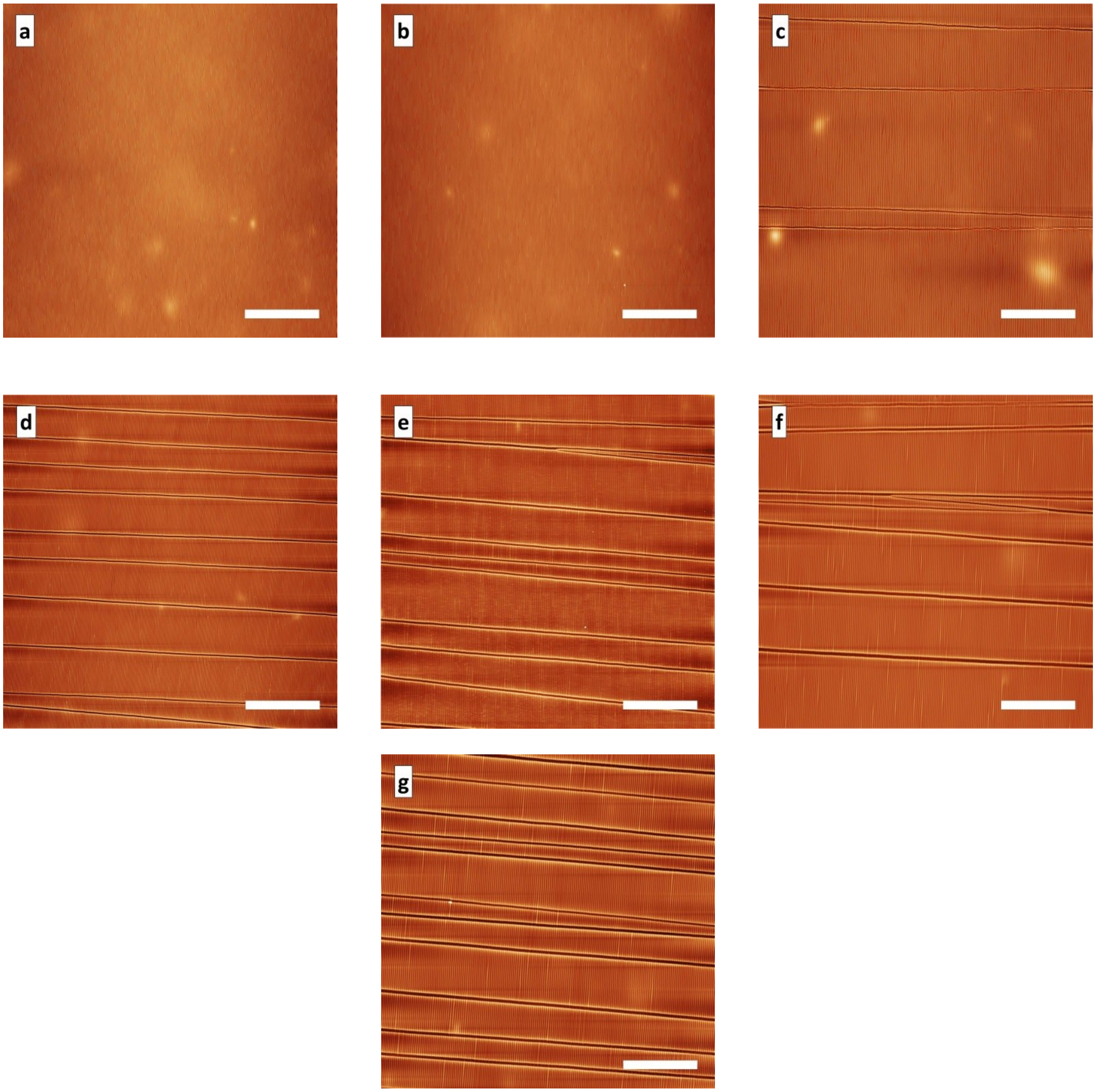

Figure S2: Topographical AFM images of the power screening, with (**a**) = 4 W, (**b**) = 8 W, (**c**) = 16 W, (**d**) = 32 W, (**e**) = 48 W, (**f**) = 64 W and (**g**) = 80 W. 10 x 10 µm cutouts are added to the power screening in Fig. 2 b. Scale bar is 20 µm.

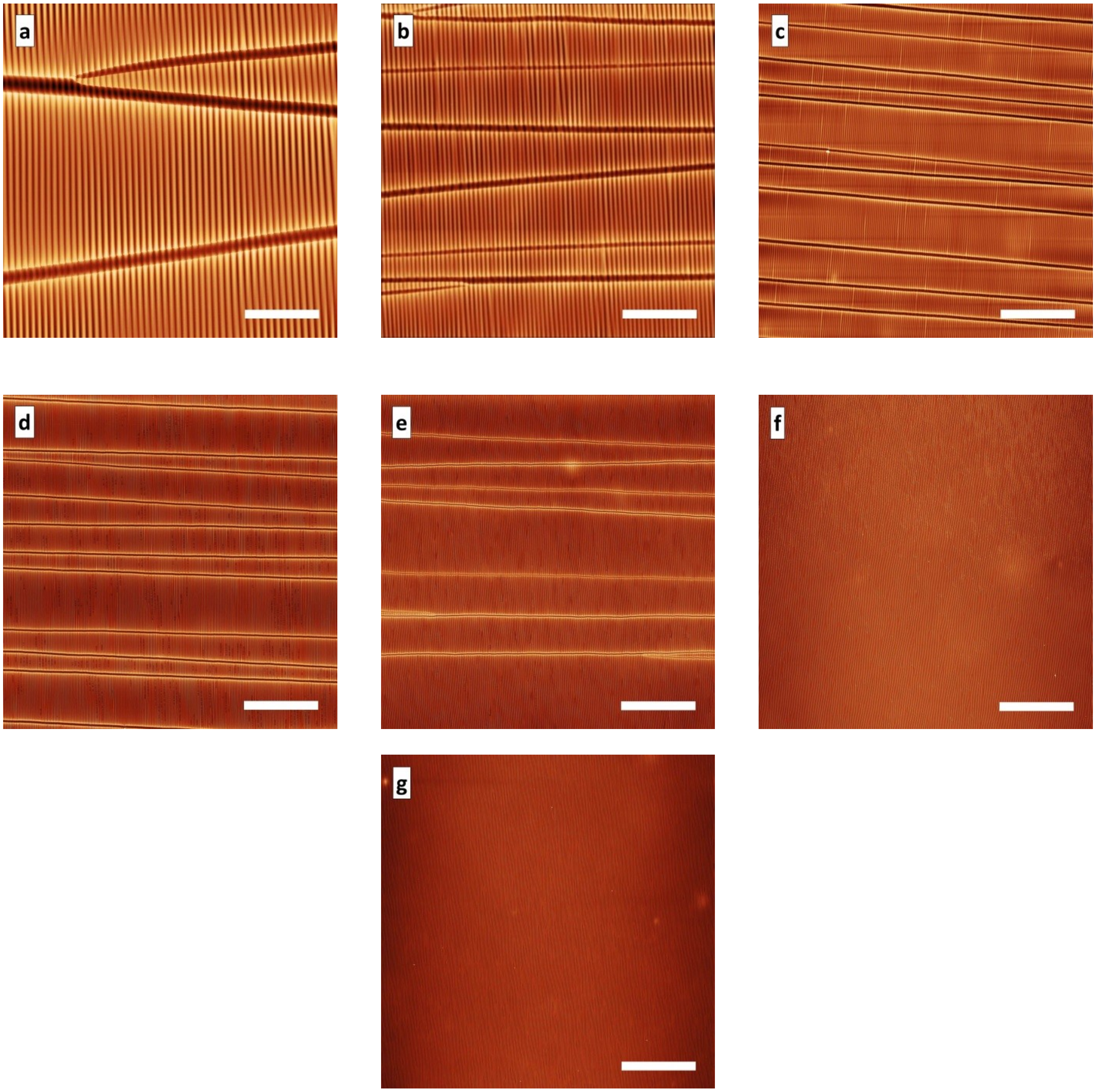

Figure S3: Topographical AFM images of the pressure screening, determined analogous to Figure S2. With (a) = 0.05 mbar, (**b**) = 0.1 mbar, (**c**) = 0.2 mbar, (**d**) = 0.3 mbar, (**e**) = 0.6 mbar, (**f**) = 0.9 mbar and (**g**) = 1.2 mbar. 10 x 10 µm cutouts are added to the pressure screening in Fig. 2 c. Scale bar is 20 µm.

Pressure	***PSD***				***2D-FT***				***Crack Density***		
	Individual		Ø		Individual		Ø		Individual	Ø	
mbar	λ **nm**	σ ± **nm**	λ **nm**	σ ± **nm**	λ **nm**	σ ± **nm**	λ **nm**	σ ± **nm**	**Area %**	**Area %**	**σ ±**
	1730,8	121,0			1710,9	24,2			7,3		
0,05	1698,1	116,5	1698,5	123,8	1697,7	30,7	1703,3	28,0	11,5	8,6	2,5
	1666,7	121,4			1701,3	26,6			7,1		
	1216,2	87,3			1217,6	22,4			7,7		
0,10	1046,5	63,2	1070,0	153,1	1040,5	16,3	1063,4	145,6	7,7	7,9	0,5
	947,4	60,9			932,0	23,1			8,5		
	514,3	29,3			511,6	15,8			7,8		
0,20	494,5	29,7	499,3	32,1	494,9	14,1	499,8	18,6	6,8	6,7	1,2
	489,1	28,9			492,8	16,5			5,3		
	454,6	22,9			454,1	14,8			4,6		
0,30	422,5	23,4	434,5	30,3	426,7	12,2	436,1	20,8	4,0	4,6	0,6
	426,5	28,0			427,6	14,3			5,3		
	350,2	16,0			359,9	10,0			4,4		
0,60	312,5	17,1	325,8	26,6	317,8	9,9	334,8	24,1	1,7	2,5	1,6
	314,7	15,4			326,8	8,4			1,6		
	305,1	21,1			304,4	11,1			0,0		
0,90	314,7	16,5	311,5	19,9	316,6	8,1	311,1	11,6	0,0	0,0	0,0
	314,7	19,8			312,3	10,4			0,0		
	258,6	19,6			259,0	5,7			0,0		
1,20	255,7	16,7	258,6	18,9	262,8	9,5	262,6	9,8	0,0	0,0	0,0
	261,6	19,7			266,0	12,2			0,0		

Table S1: Results of the pressure screening, displaying PSD (left columns), 2D-FT (middle) and the according crack density values at a time (right). For each data point, three samples were measured via AFM and analyzed with both PSD and 2D-FT. The results were averaged and the deviations summed up via Gaussian error propagation.

Power	*PSD*				*2D-FT*				*Crack Density*		
	Individual		Ø		Individual		Ø		Individual	Ø	
W	λ **nm**	σ ± **nm**	λ **nm**	σ ± **nm**	λ **nm**	σ ± **nm**	λ **nm**	σ ± **nm**	**Area %**	**Area %**	**σ ±**
5	206,9 197,4 187,9	15,8 15,9 16,2	197,4	18,6	205,0 202,6 187,8	8,2 9,8 8,8	198,5	12,9	0,0 0,0 0,0	0,0	0,0
10	204,1 211,3 200,5	20,1 16,8 15,0	205,3	18,1	209,4 209,5 202,3	7,6 8,5 8,1	207,1	9,0	0,0 0,0 0,0	0,0	0,0
20	217,4 239,0 219,8	13,7 16,2 15,3	225,4	19,2	224,3 235,2 217,8	8,0 8,0 9,5	225,8	12,2	1,0 0,0 1,7	0,9	0,8
40	238,1 250,7 244,3	14,5 14,6 14,5	244,4	17,1	237,6 251,1 244,3	8,7 7,7 8,2	244,3	12,6	4,9 4,1 4,5	4,5	0,6
60	340,9 326,1 365,9	16,6 18,4 22,4	344,3	27,7	341,9 331,6 365,2	2,0 12,2 10,3	346,2	19,0	6,1 4,4 3,8	4,7	1,2
80	436,9 471,2 456,9	27,3 28,4 26,0	455,0	32,2	434,2 476,1 457,4	15,4 15,7 20,6	455,9	27,2	6,7 4,6 4,9	5,4	1,2
100	514,3 494,5 489,1	29,3 29,7 28,9	499,3	32,1	511,6 494,9 492,8	15,8 14,1 16,5	499,8	18,6	7,8 6,8 5,3	6,7	1,2

Table S2: Results of the power screening. The results were obtained analogous to Table S1.

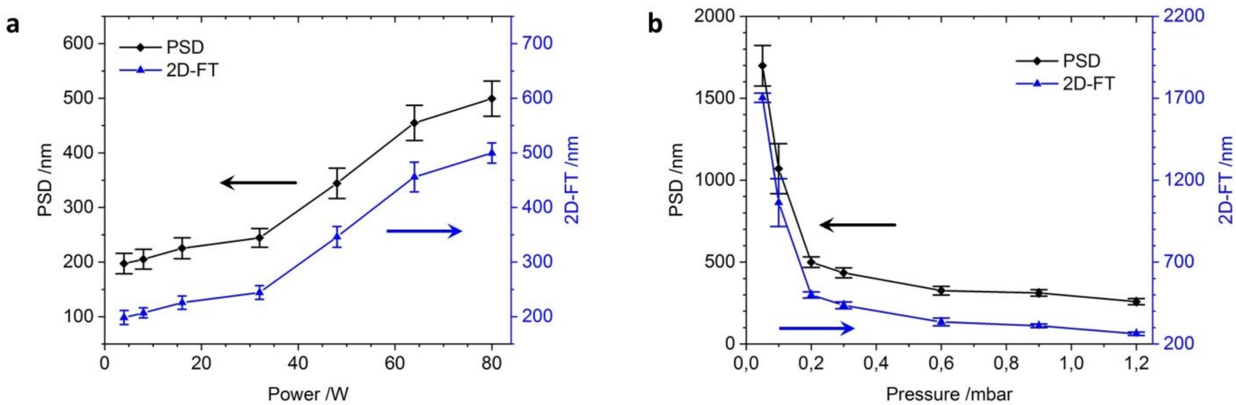

Figure S4: Wrinkle wavelengths for power (**a**) and pressure (**b**) screenings, determined via PSD (black curves) as well as 2D-FT (blue curves). PSD and 2D-FT are separated in both diagrams by an y-axis offset, since they superpose almost entirely when charting them on the same axis scale.

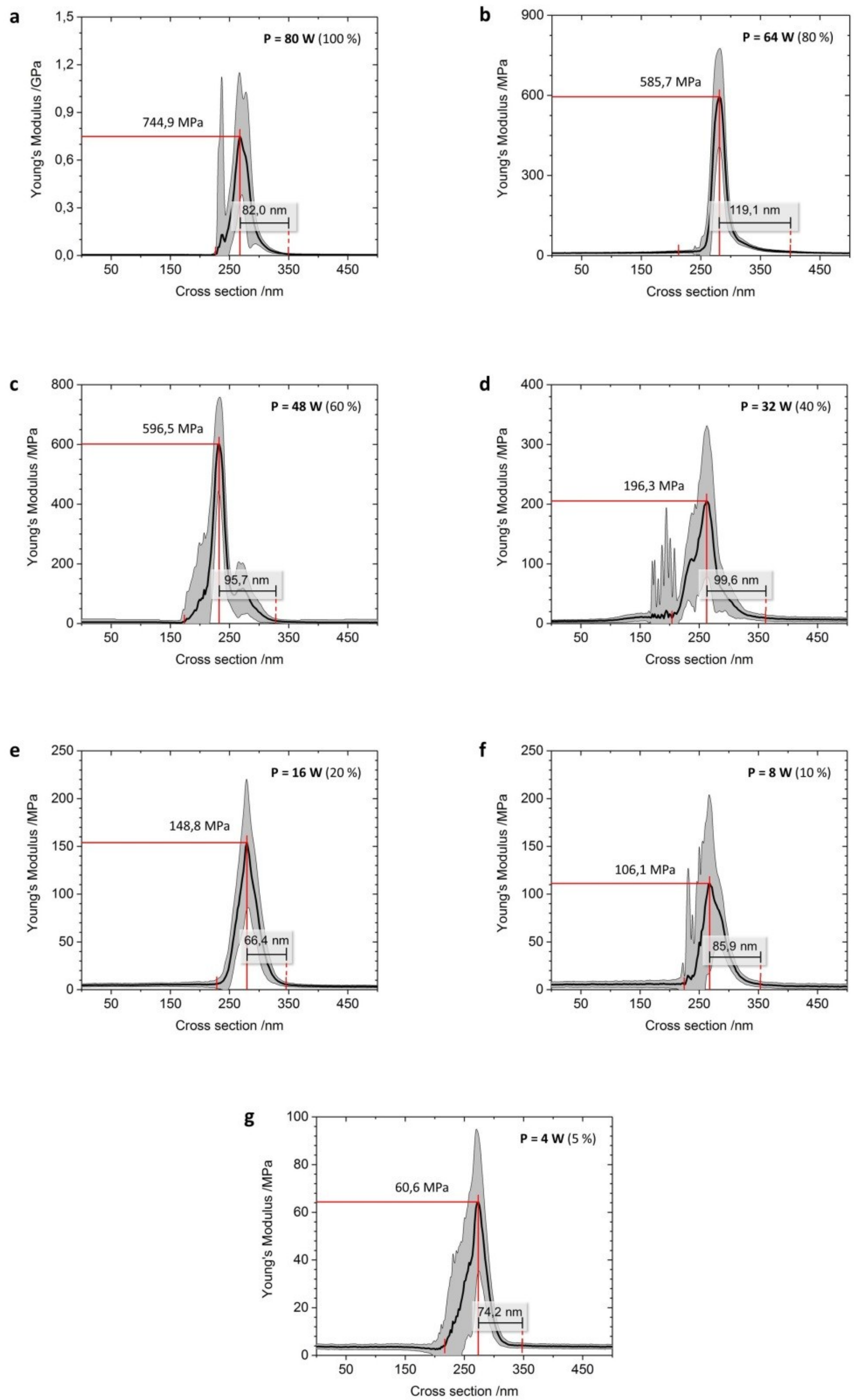

Figure S5: screening of the flat, unstrained samples, analyzed via QNM AFM method. The power range stretches from The highest accessible power at P_{max} = 80 W (**a**) to the lowest accessible power at P_{min} = 4 W (**g**). For every sample the maximum elasticity E_{max} as well as the average layer thickness t_l is denoted.

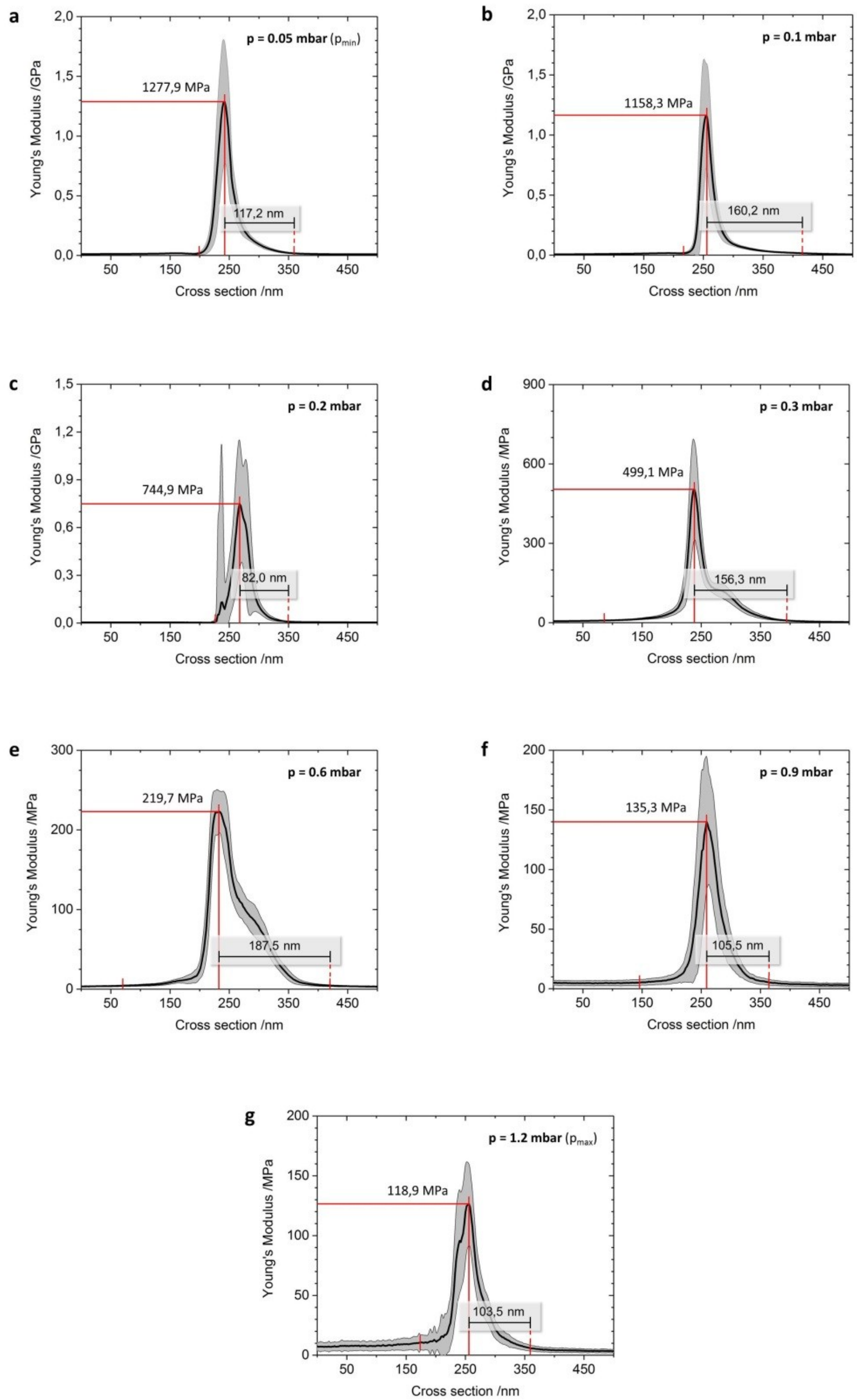

Figure S6: Pressure screening of the flat, unstrained samples, analyzed analogous to Fig. S5. The pressure range stretches from the lowest accessible pressure being p_{min} = 0.05 mbar (**a**) to the highest accessible at p_{max} = 1,2 mbar (**g**). For every sample the maximum elasticity E_{max} as well as the average layer thickness t_l is denoted.

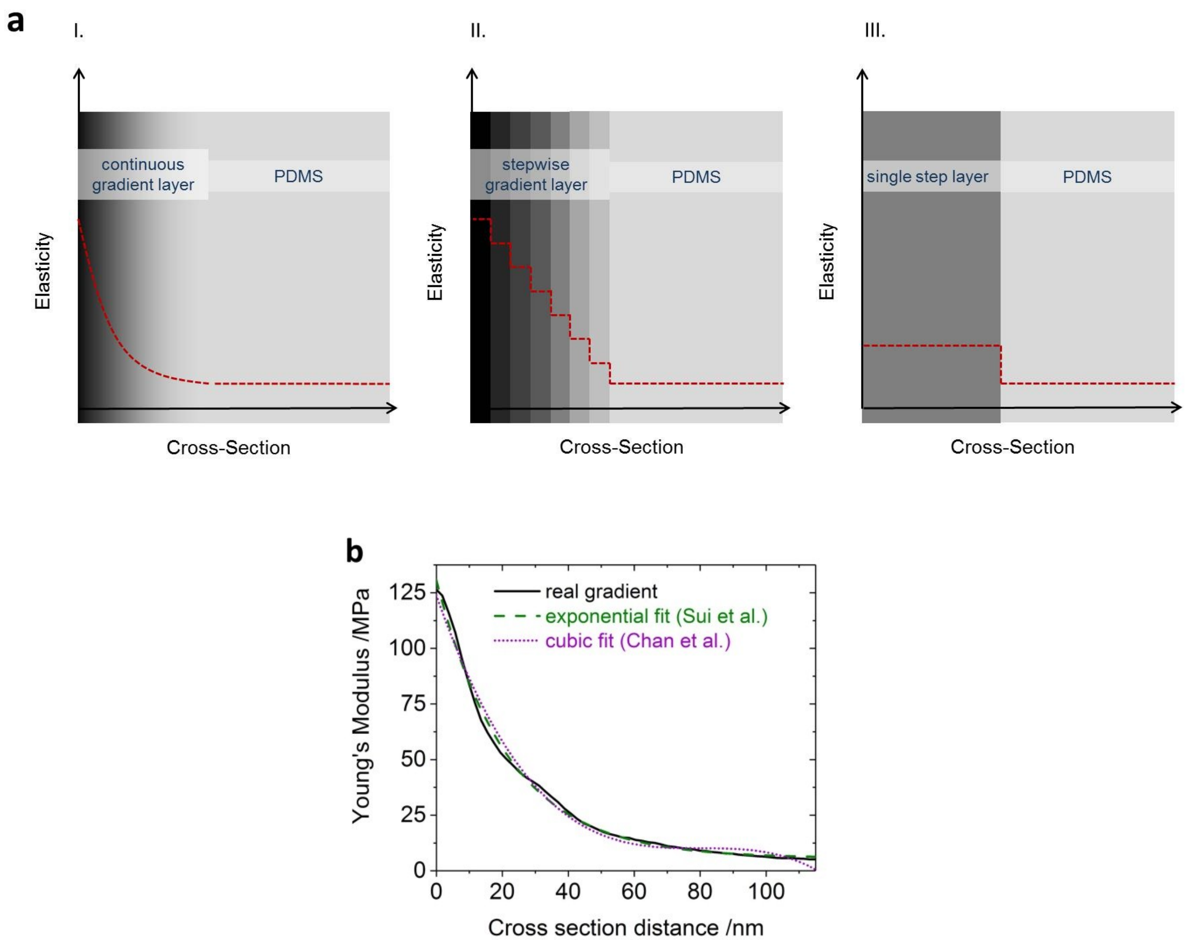

Figure S7: (**a**) Scheme of the calculated recreation of the gradient: The continuous gradient from I. is transferred into a corresponding multilayered stepwise gradient II. as well as a single step layer III. Below the corresponding stress diagrams for each layer-to-layer interface are shown schematically: For continuous (I.) and stepwise (II.) gradients a lower maximal von-Mises-stress σ_{max} than for the single step (III.) is simulated, due to the broader distribution of overall stress between layer and substrate when compared with the single layer. The critical stress σ_{crit} for cracking these layers indicates that for particular conditions $\sigma_{max,single\text{-}step} > \sigma_{crit} > \sigma_{max,gradient}$, so crack-free wrinkles can be achieved. In (**b**) the real gradient from Fig. 4 a is compared to two theoretical models; on the one hand the exponential model of Sui et al., [43] on the other hand the cubic model of Chan et al. [42] Both are in very good agreement with the experimental data, however the exponential model is even closer ($R_2 = 0.996$) than the cubic one ($R_2 = 0.990$).